

Modelling Alkali Metal Reacting Dynamics using Tabulated Detailed Sodium Chemistry in Large-Eddy Simulation of a Coflow-Heated Pulverised-Coal Jet Flame

K.D. Wan¹, J. Xia^{2,*}, L. Vervisch³, Z.H. Wang¹, K.F. Cen¹

¹ State Key Laboratory of Clean Energy Utilization, Zhejiang University, Hangzhou 310027, China

² Department of Mechanical, Aerospace and Civil Engineering & Institute of Energy Futures, Brunel University London, Uxbridge UB8 3PH, UK

³ INSA de Rouen, CORIA - CNRS & Normandie Université, 76800 Saint-Etienne-du-Rouvray, France

Abstract

In this paper a subset of a detailed sodium chemistry mechanism [1] has been tabulated and coupled with a large-eddy simulation (LES) solver to investigate alkali metal emissions during pulverised-coal combustion for the first time. The combustion-conserved equivalence ratio of the hydrocarbon-fuel/air gas mixture, a mixture fraction for sodium reactions and the gas-phase temperature have been used to define the initial conditions of chemical trajectories of sodium reactions. A progress variable has been defined to track the sodium reaction progress. A four-dimensional chemical lookup table is then built and coupled with LES of pulverised-coal combustion, where the volatile species generation is predicted in-situ by the CPD (Chemical Percolation Devolatilisation) model [2] and gas-phase reactions by the PaSR (Partially Stirred Reactors) model [3]. Characteristics of the reacting dynamics of sodium minor species in a pulverised-coal jet flame are obtained.

Introduction

Turbulent solid-fuel combustion occurs in a variety of power-generating combustion devices burning coal, biomass or their blends. Alkali metal minor-species emissions, including sodium species rich in some coal and potassium species usually rich in biomass, accelerate ash deposition on heat exchanging surfaces and degrade heat transfer efficiency, thus leading to severe operating issues of the industrial combustion devices. Modelling reacting dynamics of minor species in a turbulent multiphase flame is still an open challenge, although global combustion characteristics of a turbulent gaseous flame can be reasonably predicted nowadays. In this work a detailed sodium chemistry has been tabulated and incorporated into high-fidelity simulation of a turbulent pulverised-coal flame. This first attempt has made possible numerical experiments of minor species formation and reacting dynamics prediction in laboratory- and industrial-scale turbulent solid-fuel combustion.

Specific Objectives

In view of the research need to develop modelling approaches to tracing alkali metal minor species in turbulent solid-fuel combustion, the specific objective of this work is to evaluate detailed chemistry tabulation and its coupling with a high-fidelity multiphase flow solver. Chemistry tabulation is appealing to the community due to the low computational cost required for incorporating detailed chemistry into reacting flow simulation.

Sodium Chemistry Tabulation

The following assumptions and simplifications have been made in this work:

1. In the laboratory-scale pulverised-coal jet flame considered in this study, char combustion is limited and therefore not considered.
2. The sodium species and composition released from a pulverised-coal particle is an important initial condition. Although progress is being made (e.g. [4]), no detailed knowledge has been obtained. Therefore atomic sodium (Na) has been assumed to be the sole sodium species released from a sodium-rich pulverised-coal particle, since it was predicted to be the favoured species in a flame environment. We understand this is a strong assumption, which also facilitated the definition of a progress variable for the sodium reactions. Once a proper sodium release model is available, we can inherit the modelling approach developed here only if a proper progress variable can be found. In this respect automatic tools (e.g. [5]) to generate an optimal progress variable can be of assistance.
3. The sodium release rate, or the particle source term in the transport equation for the sodium mixture fraction Z_{Na} is proportional to the pyrolysis rate or the source terms in the transport equations for volatile species. This simplification is based on the knowledge that the sodium vapour generated inside the porous structure of a coal particle is transported outwards by the volatile produced during the pyrolysis stage.
4. In the present study, a subset of the 24 reactions in [1], including 4 elements Na, C, H and O and 5 species Na, NaO, NaO₂, NaOH and (NaOH)₂ is considered. Sulphur and Chlorine are not considered.
5. Since the magnitude of sodium species is very small and at the ppm (parts-per-million) level, it is assumed that the sodium reactions do not influence gaseous hydrocarbon volatile combustion.
6. Subgrid turbulence-chemistry interactions are not considered for sodium reactions. Therefore the source term ω_c obtained from the chemical lookup table is directly

*Corresponding author: jun.xia@brunel.ac.uk
Proceedings of the European Combustion Meeting 2017

used as the source for the transported filtered progress variable \tilde{Y}_c .

For the pulverised-coal-particle-laden jet heated by a co-flow [6], we define the initial conditions for chemical trajectories of the 5 sodium species with 3 variables:

1. The combustion-conserved equivalence ratio ϕ_{CH} for gaseous hydrocarbon fuel, defined as $\phi_{CH} = (2X_C + X_H/2)/X_O$. X_C , X_H and X_O are the mole fractions of atomic carbon, hydrogen and oxygen in the gas mixture, respectively. The mole fractions are evaluated on the LES grids using filtered mass fractions \tilde{Y}_i of gas species.

2. A mixture fraction Z_{Na} for sodium reactions, which is defined in this paper as the mass fraction Y_{eNa} of the sodium element. A filtered convection-diffusion equation is used to transport \tilde{Z}_{Na} or \tilde{Y}_{eNa} , with a source term \tilde{S}_{eNa} on the right-hand side of the equation accounting for sodium vapour released from a pulverised-coal particle, which is proportional to the volatile release rate.

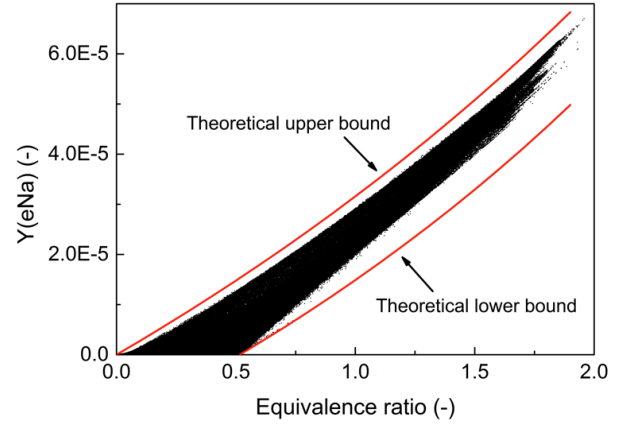
3. The gas-phase temperature T_g . The filtered gas-phase temperature \tilde{T}_g is obtained from the filtered energy equation transporting $\overline{\rho_g T_g}$ with source terms due to gas-phase combustion, radiative heat transfer and heat exchange between the gas and particle phases.

The equivalence ratio ϕ_{CH} and the sodium mixture fraction Z_{Na} are used to quantify the mixing among three feeding streams: (1) the primary pulverised-coal-particle-laden air jet, (2) the high-temperature co-flow and (3) the volatile stream originated from coal particles. Note since the release rates of volatile gas and sodium vapour are proportional to each other, Z_{Na} can be used to quantify the mixing of the volatile stream into the gas mixture.

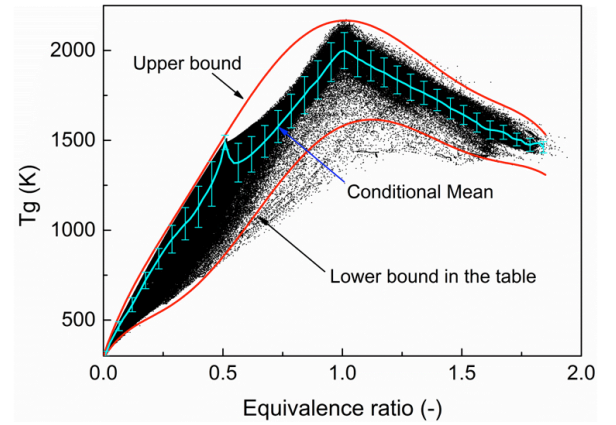
The gas-phase temperature T_g accounts for temperature effects on sodium species, including (1) temperature rise due to gas-phase combustion, (2) heat loss due to radiation and (3) heat exchange between the two phases. Note the reactions of sodium minor species have negligible effects on T_g .

Figure 1(a) shows a scatter plot of Z_{Na} against ϕ_{CH} obtained from an instantaneous LES result. The data points illustrates the mixing status among the 3 feeding streams. The theoretical upper and lower bounds of Z_{Na} can be obtained from the compositions of atomic C, H and O in the 3 feeding streams and are also shown in the figure. The 2 bounds are also used as the minimal and maximal Z_{Na} at each equivalence ratio to build the chemical lookup table. The upper bound indicates a mixture of volatile and the primary air jet, and the lower bound indicates a mixture of volatile and the hot co-flow. Since the primary air jet flow carries the particle phase, a pure mixture between volatile and the co-flow cannot form. Since volatile is generated from a pulverised-coal particle after it is heated by the co-flow, a pure mixture between volatile and the primary air jet cannot form either. Therefore both the upper and lower bounds are not reached.

Figure 1(b) shows a scatter plot of T_g against ϕ_{CH} . The conditional mean and fluctuations of the gas-phase temperature at each equivalence ratio are also shown in



(a) Sodium mixture fraction $Z_{Na}(= Y_{eNa})$ vs ϕ_{CH}



(b) Gas-phase temperature T_g vs ϕ_{CH}

Figure 1: Scatter plots of an instantaneous LES result.

the figure, together with the upper and lower bounds used to build the table. The lower bound is chosen to keep the temperature range for all the equivalence ratios less than 700 K. It can be seen that the conditional fluctuations are completely contained in the 2 bounds.

After identifying the 3 parameters which define the initial conditions of chemical trajectories of sodium species, the time evolutions of these trajectories need to be remapped into a progress variable space. A progress variable Y_c is a linear function of the mass fractions of the 5 sodium species considered in this study. It should monotonically evolve with the time t so that the mass fractions Y_i of all the sodium species can be expressed as singled-valued functions of Y_c , i.e. $Y_i(t, \xi) = Y_i[t(Y_c, \xi), \xi] = Y_i[t(Y_c), \xi] = Y_i(Y_c, \xi)$, where the initial conditions of a chemical trajectory is denoted by $\xi = \xi(\phi_{CH}, Z_{Na}, T_g)$. In addition, the gradient of the sodium species concentrations in the progress variable space $\partial Y_i(Y_c, \xi)/\partial Y_c$ should not be overly big [5]. Otherwise a small deviation in the prediction of Y_c would lead to unacceptable errors when obtaining sodium species mass fractions from the table.

In the present work, since atomic sodium Na is the assumed sodium species ejecting from a pulverised-coal particle, the total mass fractions of the sodium element in all the other 4 sodium species, including NaO,

NaO_2 , NaOH and $(\text{NaOH})_2$, should be a proper candidate for the progress variable. Since the total mass of the sodium element is conserved during sodium reactions, this progress variable should monotonically increase with the consumption of Na in time. In addition, since $Y_{(\text{NaOH})_2}$ is orders of magnitude smaller than that of the other sodium species, a large constant weighting factor (10^4) has been applied to $Y_{(\text{NaOH})_2}$ to reduce the magnitude of $\partial Y_{(\text{NaOH})_2} / \partial Y_c$, thereby improving the accuracy of the chemical table on predicting this minor sodium species.

Therefore, the progress variable Y_c is defined as

$$Y_c = Y_{c,I} + Y_{c,II}, \quad (1)$$

where

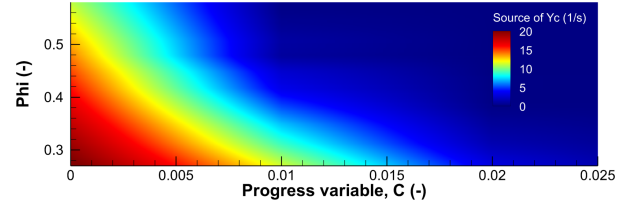
$$Y_{c,I} = \sum_i (\nu_{\text{Na},i} W_{\text{Na}} / W_i) Y_i, \quad (2)$$

$$Y_{c,II} = (\nu_{\text{Na},j} W_{\text{Na}} / W_j) Y_j \times (10^4 - 1). \quad (3)$$

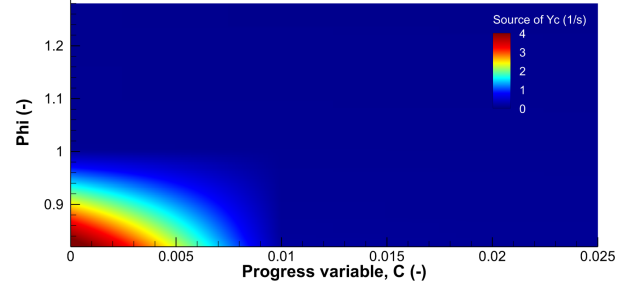
$\nu_{\text{Na},i}$ is the number of the sodium element in species i of the 4 sodium compounds, W is the molecular weight, and species j is $(\text{NaOH})_2$.

To build up the sodium chemistry table, the chemical equilibrium state of gaseous hydrocarbon combustion is first predicted using CANTERA and GRI-3.0 for each initial condition $\xi(\phi_{\text{CH}}, Z_{\text{Na}}, T_g)$, excluding sodium reactions. Then a zero-dimensional simulation of sodium reactions is run for 2.0 s, which is much longer than the residence time of a fluid particle of the jet flow, using CANTERA in combination with GRI-3.0 and the detailed sodium chemistry [1]. It is also sufficiently long for the sodium reactions reaching their chemical equilibrium states except for a limit number of cases under some low-temperature conditions. The obtained chemical trajectory can then be remapped into the progress variable space. Specifically, for each Y_c , the corresponding i -th sodium species concentration Y_i and the source term $\dot{\omega}_c$ in the transportation equation for Y_c can be obtained and are stored into the chemistry table. $\dot{\omega}_c$ is a linear combination of the source for Y_i with the same weighting factors as in Eq. 2. Y_c is normalised by the final maximal value before stored in the table. The normalised progress variable $C(t, \xi) = Y_c(t, \xi) / Y_{c,\max}(2.0, \xi)$ monotonically evolves from 0 to 1 for any single chemical trajectory of the sodium reactions.

The equivalence ratio ϕ_{CH} , varying in $[0, 1.85]$, is discretised on a 100 nonuniform grid, with refined grid points around $\phi_{\text{CH}} = 1.0$ where the sodium species concentrations vary rapidly. 30 and 50 uniform grid points are used for Z_{Na} and T_g , respectively. 100 grid points are allocated for the normalised progress variable C , and the grid is refined for small C values at the initial stage of the sodium reactions. The sodium chemistry database has therefore $\phi_{\text{CH}} \times Z_{\text{Na}} \times T_g \times C = 100 \times 30 \times 50 \times 100$ coordinates in total, on each of which the 5 sodium species mass fractions and $\dot{\omega}_c$ are stored. The size of this complete table is 700 MB.

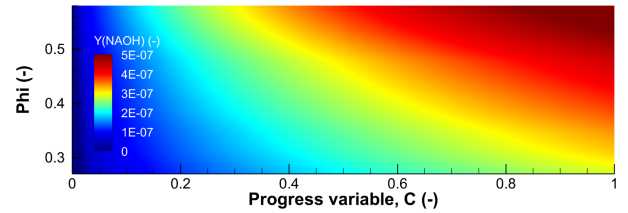


(a) $T_g = 1,000\text{K}$, $Y_{\text{eNa}} = 5 \times 10^{-6}$, $0.27 \leq \phi_{\text{CH}} \leq 0.58$.

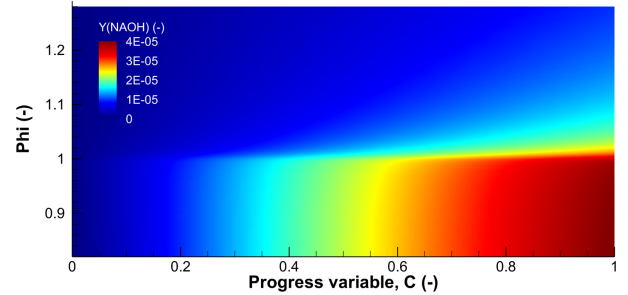


(b) $T_g = 1,700\text{K}$, $Y_{\text{eNa}} = 2.5 \times 10^{-5}$, $0.82 \leq \phi_{\text{CH}} \leq 1.28$.

Figure 2: Sample contours of the progress variable source $\dot{\omega}_c$ stored in the table at a (a) low and (b) high gas-phase temperature.



(a) $T_g = 1,000\text{K}$, $Y_{\text{eNa}} = 5 \times 10^{-6}$, $0.27 \leq \phi_{\text{CH}} \leq 0.58$.



(b) $T_g = 1,700\text{K}$, $Y_{\text{eNa}} = 2.5 \times 10^{-5}$, $0.82 \leq \phi_{\text{CH}} \leq 1.28$.

Figure 3: Sample contours of NaOH mass fractions Y_{NaOH} stored in the table at a (a) low and (b) high gas-phase temperature.

Figure 2 shows sample contours of the progress-variable source $\dot{\omega}_c$ stored in the table at a low [1,000 K; Fig. 2(a)] and high [1,700 K; Fig. 2(b)] gas-phase temperature for $C \in [0, 0.025]$. $\dot{\omega}_c$ is relatively small, although nonzero, and therefore not shown for $C \in [0.025, 1]$. At $T_g = 1,000\text{K}$, the gaseous mixture is always fuel-lean. For a fuel-lean mixture, $\dot{\omega}_c$ is large at the early stage of the chemical trajectories due to fast oxidation of Na towards NaO_2 , and decreases as the sodium reactions progress. $\dot{\omega}_{c,C=0}$ increases as ϕ_{CH} decreases. Figure 3 shows sample contours of the mass fraction of an impor-

tant sodium species NaOH stored in the table at the two temperatures. NaOH will be continuously produced as the sodium reactions progress towards the equilibrium, and more NaOH, although on the same order of magnitude, will be produced if the gaseous mixture contains more hydrocarbon fuel. At the higher gas-phase temperature $T_g = 1,700\text{K}$, a similar trend can be identified for a fuel-lean mixture. For a fuel-rich mixture, however, the production of NaOH tends to slow down.

The sodium chemistry table has been comprehensively validated by comparing the sodium species mass fractions predicted by the table and by the detailed sodium chemistry directly, given a specified initial condition $\xi(\phi_{\text{CH}}, Z_{\text{Na}}, T_g)$.

The chemical lookup table, which is based on trajectories obtained at a fixed value of the gas-phase temperature T_g , cannot account for the variations of the sodium compositions at a chemical equilibrium state due to the variation of T_g . $\dot{\omega}_c^{\text{RTE}}$ has therefore been used as a relaxation towards the new equilibrium conditions [7],

$$\dot{\omega}_c^{\text{RTE}} = \frac{Y_c^{\text{EQ}}(\phi_{\text{CH}}, \tilde{Z}_{\text{Na}}, \tilde{T}_g) - \tilde{Y}_c}{\gamma \delta t}, \quad (4)$$

where δt is the time step; γ is a relaxation coefficient and set to be 1 in this work. Therefore

$$\tilde{\omega}_c = \dot{\omega}_c^{\text{TAB}}(\phi_{\text{CH}}, \tilde{Z}_{\text{Na}}, \tilde{T}_g) + \beta \dot{\omega}_c^{\text{RTE}}, \quad (5)$$

where $\beta = 0$ if the sodium reactions have not reached chemical equilibrium, i.e. $\tilde{Y}_c < Y_c^{\text{EQ}}$. Otherwise $\beta = 1$. $\dot{\omega}_c^{\text{TAB}}$ is the source term obtained from the table.

Volatile Pyrolysis and Combustion Models

Volatile species prediction is crucially important for key pulverised-coal combustion characteristics such as ignition and the liftoff height. In this study an advanced pyrolysis model CPD has been incorporated into an LES solver [8] to predict gaseous volatile species production from a pulverised-coal particle according to the local heating rate, thereby improving modelling of coal pyrolysis over a wide range of operating conditions [9].

The filtered reaction rate $\bar{\omega}_i$ is calculated by the PaSR model. PaSR has been applied to LES of both non-premixed [3] and premixed [10] combustion. Each LES grid cell is viewed as a partially stirred reactor containing fine structures where mixing and reaction occur and the surroundings dominated by large-scale flow structures. $\bar{\omega}_i = \kappa \dot{\omega}_i(\bar{\rho}_g, \bar{Y}_i, \bar{T}_g)$, where κ is the reacting volume fraction, defined by the ratio between the volume swept by the reacting structures and the volume swept by mixing and reacting structures. It is therefore can be estimated by $\kappa = \tau_c / (\tau_c + \tau_m)$, where τ_m and τ_c are a subgrid mixing time scale and a chemical time scale, respectively. In this work τ_m is approximated by the harmonic mean of the smallest Kolmogorov time scale τ_K and the largest subgrid time scale τ' in a LES filtering volume; And the characteristic chemical time scale τ_c is estimated by a laminar

flame thickness divided by a laminar flame speed.

LES Two-Phase Flow Solver

The filtered Navier-Stokes equations in the low-Mach-number form for mass, momentum, species mass and temperature are solved for the gas phase. The sub-grid scale flow terms are computed by the Germano model. In addition to volatile species and their combustion products with air, \tilde{Z}_{Na} and \tilde{Y}_c are also transported. For the sodium mixture fraction \tilde{Z}_{Na} , there is a particle source but no reaction source in its transport equation. While for the progress variable \tilde{Y}_c , there is a reaction source, which is obtained from the sodium-chemistry table, but no particle source. Pulverised-coal particles are modelled as point sources and full two-way coupling between the gas and particle phases due to pyrolysis, combustion and heat exchange between the two phases including radiation has been incorporated.

A 2nd-order Crank-Nicolson scheme is used for time advancement. A 3rd-order weighted essentially non-oscillatory (WENO) scheme is used for scalar advection in the species and temperature equations, while a 2nd-order central difference scheme for scalar diffusion in the species and temperature equations and all the terms in the momentum equation.

The LES solver has been validated on a particle-laden turbulent air jet [8], pilot-assisted [11] and coflow-heated [12] pulverised-coal combustion.

The software package has been optimised on the UK national supercomputer ARCHER [13]. The load balance of particles has been achieved via on-the-fly redistributing particles among all the cores. In addition, using one-sided MPI communication instead of collective MPI communication has greatly enhanced the parallel efficiency of redistributing particles among cores.

Results and Discussion

A coflow-heated pulverised-coal jet flame [6] has been simulated and the LES results validated [12]. For the case reported here, the setup is the same as that of the inlet stoichiometric ratio 0.22 [6], except that we have used properties of Loy Yang brown coal, for which sodium data are available.

Two-dimensional snapshots of the 4 variables, i.e. C , ϕ_{CH} , Z_{Na} and T_g , which are the 4 coordinates of the chemical lookup table, are shown in Fig. 4. Pulverised-coal particles, which are carried by the cold primary air jet, are heated by the high-temperature co-flow and release volatile as pyrolysis continues. Volatile gas then burns around coal particles, thereby enhancing pyrolysis and helping achieve stable ignition and combustion of the pulverised-coal jet. Since the equivalence ratio ϕ_{CH} is 0 for the primary air jet and relatively low ($= 0.52$) for the co-flow, the regions where large ϕ_{CH} values are found is where volatile is generated from heated coal particles, and therefore also is where the sodium element mass fraction $Y_{\text{eNa}} (= Z_{\text{Na}})$ is big due to the direct relationship between the production rates of sodium vapour and volatile.

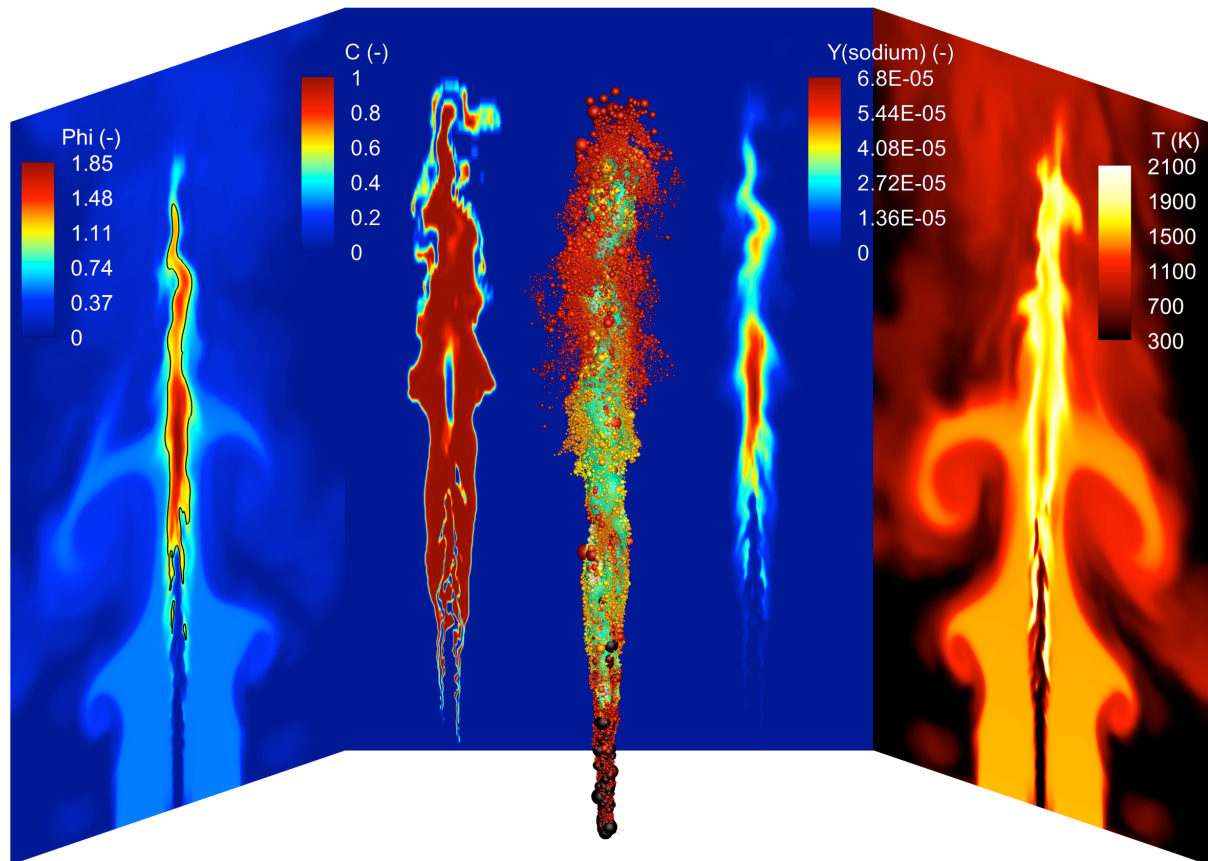


Figure 4: Sodium chemistry tabulation in LES of a weakly turbulent coflow-heated pulverised-coal jet flame. The four planes show a snapshot of the equivalence ratio ϕ_{CH} (black solid: $\phi_{CH} = 1$), the normalised progress variable C , the mass fraction of the sodium element Y_{eNa} , and the gas-phase temperature T_g ; the four coordinates of the chemical lookup table for a subset of a detailed sodium chemistry. The three-dimensional plot shows the coal-particle distribution with particle size and temperature information and the $Y_{NaOH} = 2 \times 10^{-5}$ iso-surface.

Figure 5 shows instantaneous mass fractions of the 5 sodium species. It can be seen from Fig. 5(a) that the atomic sodium Na features a higher concentration in fuel-rich regions, since Na is the assumed outgassing species released along with the volatiles from coal particles. NaOH is formed in both fuel-lean and fuel-rich regions. The highest Y_{NaOH} is found close to the stoichiometry $\phi_{CH} = 1$. NaO is found to be produced under the stoichiometric condition, but the magnitude of its mass fraction is two orders lower than those of Na and NaOH. Both NaO_2 [Fig. 5(d)] and $NaOH_2$ [Fig. 5(e)] are generated under fuel-lean conditions. However, the concentration of NaO_2 reaches a considerably higher value near the ignition region of the pulverised-coal jet flame - a flow zone where sodium vapour is already generated from coal particles, but the temperature is still low. Finally, the concentration of $(NaOH)_2$ is very low in the whole domain.

Conclusions and Outlook

Tabulating a (subset of) detailed sodium chemistry and coupling it with a LES solver has been attempted for turbulent pulverised-coal combustion. This method provides a possibility of predicting formation and reacting

dynamics of minor species in a complex turbulent multiphase flame using high-fidelity simulation at a reasonable computational cost. The onsite table size is 700/6 MB. One more dimension or coordinate (e.g. due to char combustion) for the table would make direct loading of the table onto each compute core during simulation difficult. Characteristics of sodium species in a pulverised-coal flame predicted by the developed methodology remains to be validated against measurement, which is currently unavailable and being planned by ZHW's group at Zhejiang University. Performance comparison between a tabulated and reduced detailed chemistry, the latter case requiring directly transporting these minor species at a higher computational cost, will be interesting.

Acknowledgements

This work was performed by KDW when he was a Research Assistant at Brunel University London. This paper was adapted by JX according to [12].

Financial support from the Royal Society and the Engineering and Physical Sciences Research Council (EPSRC) of the UK is gratefully acknowledged.

Special thanks are due to Prof. Peter Glarborg of the Technical University of Denmark, who provided us the

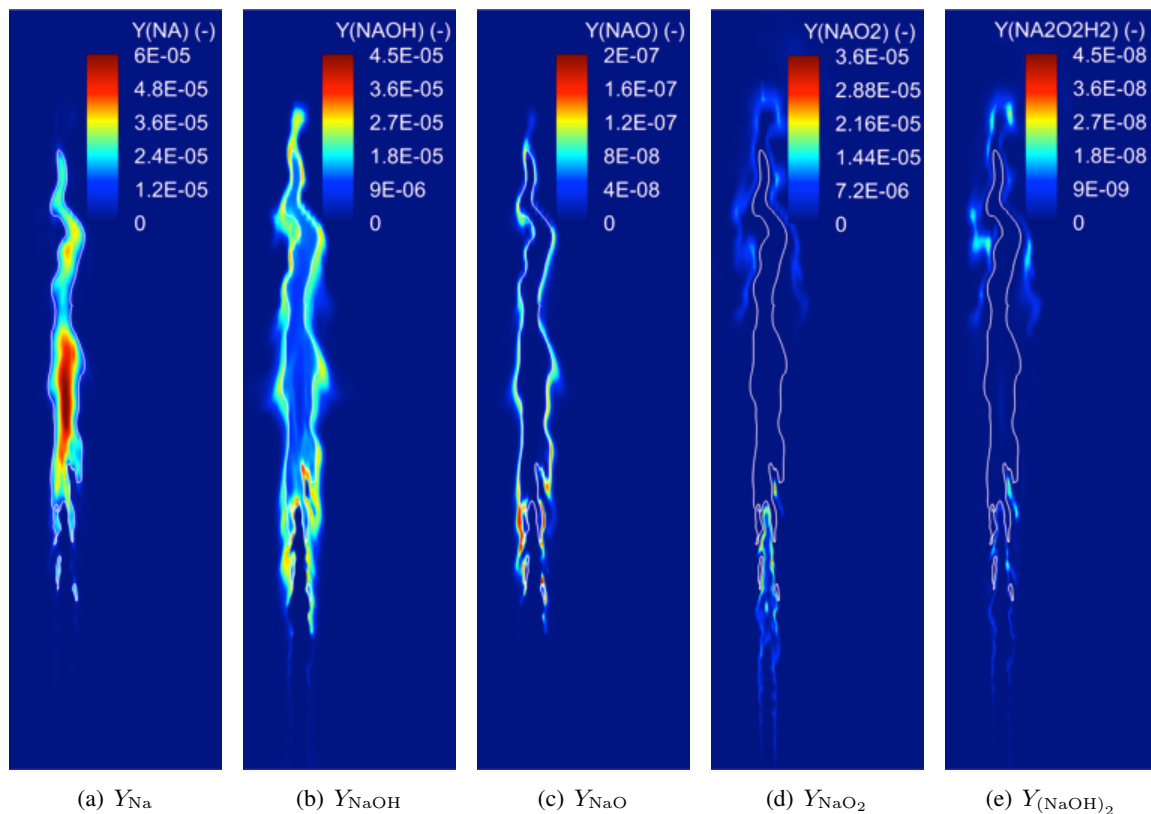


Figure 5: Sodium species distributions in a pulverised-coal jet flame. The white solid line indicates $\phi_{CH} = 1$.

detailed chemical mechanism of alkali metal species.

This work used the ARCHER UK National Super-computing Service (<http://www.archer.ac.uk>).

References

- [1] P. Glarborg, P. Marshall, Mechanism and modeling of the formation of gaseous alkali sulfates, *Combust. Flame* 141 (2005) 22–39.
- [2] D.M. Grant, R.J. Pugmire, T.H. Fletcher, A.R. Kerstein, Chemical model of coal devolatilization using percolation lattice statistics, *Energy Fuels* 3 (1989) 175–186.
- [3] M. Berglund, E. Fedina, C. Fureby, J. Tegnér, V. Sabel'nikov, Finite rate chemistry large-eddy simulation of self-ignition in supersonic combustion ramjet, *AIAA J.* 48 (2010) 540–550.
- [4] Z.H. Wang, Y.Z. Liu, R. Whiddon, K.D. Wan, Y. He, J. Xia, K.F. Cen, Measurement of atomic sodium release during pyrolysis and combustion of sodium-enriched Zhundong coal pellet, *Combust. Flame* 176 (2017) 429–438.
- [5] Y.S. Niu, L. Vervisch, P.D. Tao, An optimization-based approach to detailed chemistry tabulation: Automated progress variable definition, *Combust. Flame* 160 (2013) 776–785.
- [6] M. Taniguchi, H. Okazaki, H. Kobayashi, S. Azuhata, H. Miyadera, H. Muto, T. Tsumura, Pyrolysis and ignition characteristics of pulverized coal particles, *J. Energy Resour. Technol.* 123 (2001) 32–38.
- [7] J. Galpin, A. Naudin, L. Vervisch, C. Angelberger, O. Colin, P. Domingo, Large-eddy simulation of a fuel-lean premixed turbulent swirl-burner, *Combust. Flame* 155 (2008) 247–266.
- [8] K.D. Wan, J. Xia, Z.H. Wang, L.C. Wrobel, K.F. Cen, Online-CPD-coupled large-eddy simulation of pulverized-coal pyrolysis in a hot turbulent nitrogen jet, *Combust. Sci. Tech.* 189 (2017) 103–131.
- [9] K.D. Wan, Z.H. Wang, Y. He, J. Xia, Z.J. Zhou, J.H. Zhou, K.F. Cen, Experimental and modeling study of pyrolysis of coal, biomass and blended coal-biomass particles, *Fuel* 139 (2015) 356–364.
- [10] V. Sabelnikov, C. Fureby, LES combustion modeling for high Re flames using a multi-phase analogy, *Combust. Flame* 160 (2013) 83–96.
- [11] K.D. Wan, J. Xia, Z.H. Wang, M. Pourkashanian, K.F. Cen, Large-eddy simulation of pilot-assisted pulverized-coal combustion in a weakly turbulent jet, *Flow Turbul. Combust.*, revision submitted.
- [12] K.D. Wan, J. Xia, L. Vervisch, Y.Z. Liu, Z.H. Wang, K.F. Cen, Modeling alkali metal emissions in large-eddy simulation of a preheated pulverized-coal turbulent jet flame using tabulated chemistry, *Combust. Theory Modelling*, under review.
- [13] K.D. Wan, J. Xia, N. Banglawala, Z.H. Wang, K.F. Cen, Optimisation of LESsCOAL for large-scale high-fidelity simulation of coal pyrolysis and combustion, ARCHER eCSE05-13 Technical Report, Edinburgh Parallel Computing Centre (EPCC), Edinburgh, UK, 2017.